Whales, lifespan, phospholipids, and cataracts

Douglas Borchman,[1,*] Raphaela Stimmelmayr,[†,§] and J. Craig George[†]

Department of Ophthalmology and Visual Sciences, University of Louisville,* Louisville, KY; Department of Wildlife Management,[†] North Slope Borough, Utqiagvik, AK; and Institute of Arctic Biology,[§] University of Alaska Fairbanks, Fairbanks, AK

Abstract **This study addresses the question: why do rats get cataracts at 2 years, dogs at 8 years, and whales do not develop cataracts for 200 years? Whale lens lipid phase transitions were compared with the phase transitions of other species that were recalculated. The major phospholipids of the whale lens were sphingolipids, mostly dihydrosphingomyelins with an average molar cholesterol/phospholipid ratio of 10. There was a linear correlation between the percentage of lens sphingolipid and lens lipid hydrocarbon chain order until about 60% sphingolipid. The percentage of lens sphingolipid correlated with the lens lipid phase transition temperature. The lifespan of the bowhead whale was the longest of the species measured and the percentage of whale lens sphingolipid fit well in the correlation between the percentage of lens sphingolipid and lifespan for many species. In conclusion, bowhead whale lens membranes have a high sphingolipid content that confers resistance to oxidation, allowing these lenses to stay clear relatively longer than many other species. The strong correlation between sphingolipid and lifespan may form a basis for future studies, which are needed because correlations do not infer cause. One could hope that if human lenses could be made to have a lipid composition similar to whales, like the bowhead, humans would not develop age-related cataracts for over 100 years.**—Borchman, D., R. Stimmelmayr, and J. C. George. **Whales, lifespan, phospholipids, and cataracts.** ***J. Lipid Res.*** **2017.** 58: **2289–2298.**

Supplementary key words Cetacean • lens • lipids • bowhead whale • *Balaena mysticetus*

The purpose of the lens is to focus light on the retina. Cataract, an opacity of the lens, is the leading cause of blindness in the world for which there is no cure (1). Age is by far the biggest risk factor for each of the major causes of nonrefractive visual impairment even after adjusting for all major covariates (1). One may ask the question, why do rats get cataracts at 2 years, dogs at 8 years, and humans at 60 years? Although factors such as protein oxidation (2, 3) and cation levels (4, 5) may contribute to cataract, part of the answer is that changes in lipid composition and membrane structure may also contribute to lens opacity as reviewed in this journal (6) and others (7–10). The lipid changes with age are exacerbated with cataract (6, 9) and the total amount of glycerophospholipids is much less with age (9, 11) and in cataractous lenses and the relative amount of sphingolipids is greater compared with clear lenses (9). There is no turnover of phospholipids in the human lens (12). The changes in lipid composition with age and cataract are due to the preferential oxidation of glycerophospholipids, which, as stated below, is detrimental to the lens. Lens sphingolipids are three to four times more saturated than glycerolipids (13, 14) and, consequently, they resist oxidation more effectively than unsaturated lipids (15, 16–20). Over 90% of reactive oxygen species in the lens (16, 19) originates in the mitochondria (21–23).

There is no turnover of lipids or proteins in the lens (12, 24), so oxidative damage to lipids accumulates in the lens with age and disrupts the crystalline structure of the lens resulting in light scattering. In the human lens, the concentration of malondialdehyde, a product of lipid oxidation, increases with age (25) and cataract formation (26–33). The association between lipid oxidation and lens opacity is very strong and has led many to state that lipid oxidation may be an initiating step in the pathogenesis of human cataract (25–33). Over a human lifetime, more than 40% of the lens phospholipids are degraded forming deleterious oxidation products, and with cataract formation even more degradation occurs (9). Products of lipid oxidation impede membrane function and alter relevant cellular processes, such as growth, respiration, ATPase, and phosphate transport, as well as DNA, RNA, and protein synthesis (34).

Age-related changes in human lens lipid composition are not only associated with lens opacity, but may also reflect systemic oxidative insult, providing an indication of the health of an individual (35). Lifespan, age, and cataract are related! In general, age-related cataracts may reflect systemic factors associated with heart disease, cancer, diabetes,

This study was funded by qualified outer continental shelf oil and gas revenues, a substantial grant from the Coastal Impact Assistance program, U.S. Fish and Wildlife Service, U.S. Department of the Interior, and an unrestricted grant from Research to Prevent Blindness.

Manuscript received 21 July 2017 and in revised form 4 October 2017.

Published, JLR Papers in Press, October 16, 2017
DOI https://doi.org/10.1194/jlr.M079368

Abbreviations: DHSM, dihydrosphingomyelin; PC, phosphatidylcholine; $\tilde{\nu}_{sym}$, frequency of the symmetric CH_2 stretching band near 2,850 cm^{-1}; ΔH, change in enthalpy; ΔS, change in entropy.

[1] To whom correspondence should be addressed.
e-mail: Borchman@louisville.edu

The online version of this article (available at http://www.jlr.org) contains a supplement.

and advanced age (36). In the context of lipid changes, cataract formation appears to be an exacerbation of the aging process, and a marker of it (9). There is a 2-fold increase in mortality risk associated with both lens opacity (36–38) and cataract surgery (39–43). Lens opacity is most likely a marker of morbidity and mortality rather than a cause (42, 44). The risk of mortality is related to the type of cataract (36, 42–48). Thus, lens lipids may serve as markers for accelerated mortality (43).

Lipid oxidation is obviously deleterious to the lens and, based on inter-species differences in lens phospholipid composition, it has been suggested that humans have adapted so that their lens membranes have a high sphingolipid (lower amount of double bonds) content that confers resistance to oxidation, allowing their lenses to stay clear for a longer time relative to those in many other species (35). However, humans were the only species tested that have a lifespan of over 70 years, so to further test the idea above, in this study we measured membrane lipid structure and the phospholipid composition of bowhead whale lenses. Bowhead whales (*Balaena mysticetus*) may be the oldest mammals that exist with lifespans of over 200 years (49–54) and do not get cataracts (55). Differences in animal lens lipid composition could explain why lanosterol ameliorates cataracts in dogs and rabbits (56), but is ineffective in reversing cataracts in humans (57).

METHODS

Sample collection

For several decades, scientists with the North Slope Borough Department of Wildlife Management have worked closely with Eskimo whaling captains from the 11 Alaskan whaling communities to examine bowhead whales taken during subsistence hunts (58). Aboriginal bowhead whale hunting occurring during spring and fall in 11 Alaskan whaling communities has been regulated by a quota system under the authority of the International Whaling Commission since 1977. During this longstanding cooperative research relationship, a large number of eyes from freshly dead whales have been preserved (frozen intact at −20°C) along with other tissue samples and basic biological data for each whale. Marine mammal tissue samples used in this study were collected under National Marine Fisheries Service permits 17350-00 and 17350-01 issued to the North Slope Borough Department of Wildlife Management.

Globe enucleation, lens dissection, and lipid extraction

Unlike globe enucleation from humans and animals obtained from the local abattoir, whose death and globe dissection occur at room temperature, whales globes were harvested in ideal conditions. The ambient air and water temperature at the time of the whale harvest was at or below freezing. From time of death to sample collection (i.e., whales landed) it took on average 5–6 h. A scientist was present to remove the globe immediately upon landing and the globe was one of the first of the tissues collected. Previously frozen whale lenses were removed from the globe by an anterior approach. The iris and ciliary body were carefully removed from the lens by cutting the zonules with curved micro scissors.

Lenses were each extracted using a monophasic methanol extraction procedure that gave the highest yield of lens phospholipid compared with other extraction protocols (59). Lenses were each added to 5 ml of methanol (Sigma-Aldrich, St. Louis, MO) in a 25 ml glass scintillation vial (Fisher Scientific, Pittsburgh, PA) and chopped using a Teflon™ coated spatula. Argon gas (analyzed, ultra-pure; Welders Supply, Louisville, KY) was bubbled into the methanol/lens mixture for 2 min to remove oxygen. The vial was sonicated in an ultrasonic bath (model 1510; Branson Ultrasonics, Danbury, CT) for 10 min. The mixture was centrifuged for 10 min at 10,000 *g*. The supernatant was decanted and dried with a stream of argon gas. Methanol (5 ml) was added to the pellet and the procedure above, from the bubbling of argon gas on, was repeated two times with the supernatant from the centrifugation step added to the supernatant(s) from the previous steps and dried with a stream of argon gas. To ensure all methanol was removed from the sample, it was dried further in a lyophilizer set at 29 torr and a condenser temperature <−50°C (Labconco, Kansas City, MO; Freeze Dryer 3) for 1 h. $CDCl_3$ (1 ml; Sigma-Aldrich) was added to the dried lipid. The vial was sonicated in an ultrasonic bath (model 1510; Branson Ultrasonics, Danbury, CT) for 10 min and the mixture was placed into a 9 mm microvial with a Teflon™ cap (Microliter Analytical Supplies, Suwanee, GA) to which argon gas was added. Samples were stored for no more than 24 h at −20°C.

Cholesterol to phospholipid ratio analysis using ^{1}H-NMR

Half (500 µl) of the lens lipid-$CDCl_3$ extract was transferred from the microvial to an NMR tube using a glass pipette. Spectral data were acquired using a Varian VNMRS 700 MHz NMR spectrometer (Varian, Lexington, MA) equipped with a 5 mm $^{1}H\{^{13}C/^{15}N\}^{13}C$ enhanced PFG cold probe (Palo Alto, CA). Spectra were acquired with a minimum of 250 scans, 45° pulse width, and a relaxation delay of 1.0 s. All spectra were obtained at 25°C. Spectra were processed and integration of spectral bands was performed with GRAMS/386 software (Galactic Industries, Salem, NH). Cholesterol to phospholipid molar ratios were calculated as discussed in the Results.

Measurement of phospholipid composition using ^{31}P-NMR

A methanol/0.2 M Cs-EDTA (4:1) reagent (60) was added (250 µl) to the sample used for ^{1}H-NMR spectroscopy and homogenized with the use of a temperature-controlled ultrasonic bath at 40°C for 10 min. ^{31}P-NMR spectra were measured using a Varian Inova-400 spectrometer. The parameters to perform the acquisitions were similar to those described previously (61). Briefly, a spectral width of 2,024.7 Hz (sweep width δ = 10 ppm), 60° pulse, 4,000 data points, 1.0 s delay time, 0.711 s acquisition time, and proton decoupling (WALTZ) at 500.16 MHz were used. A line broadening of 3.0 Hz and phase correction were used to process the spectra. Chemical shifts were referenced to internal or added bovine brain sphingomyelin (SM) (Sigma-Aldrich) resonance at δ = −0.09 ppm. Spectra were processed and integration of spectral bands was performed with GRAMS/386 software (Galactic Industries, Salem, NH).

Measurement of lipid phase transitions using Fourier transform infrared spectroscopy

The 500 µl of sample not used for NMR analysis was applied to an AgCl infrared window. The solvent was evaporated under a stream of argon gas and the window was placed in a lyophilizer for 4 h to remove all traces of solvent. Infrared spectra were measured using a Fourier transform infrared spectrometer (Nicolet 5000 Magna Series; Thermo Fisher Scientific, Inc., Waltham, MA). Lipid on the AgCl window was placed in a temperature-controlled infrared cell. The cell was jacketed by an insulated water coil connected to a

circulating water bath (model R-134A; Neslab Instruments, Newton, NH). The sample temperature was measured and controlled by a thermistor touching the sample cell window. The water bath unit was programmed to measure the temperature at the thermistor and to adjust the bath temperature so that the sample temperature could be set to the desired value. The rate of heating or cooling (1°C/15 min) at the sample was also adjusted by the water bath unit. Temperatures were maintained within ±0.01°C. Exactly 100 interferograms were recorded and averaged. Spectral resolution was set to 1.0 cm^{-1}. Infrared data analysis was then performed (GRAMS/386 software; Galactic Industries, Salem, NH). The frequency of the symmetric CH_2 stretching band near 2,850 cm^{-1} ($\tilde{\nu}_{sym}$) was used to estimate the content of *trans* and *gauche* rotamers in the hydrocarbon chains. The $\tilde{\nu}_{sym}$ was calculated by first baseline leveling the OH-CH stretching region between 3,500 and 2,700 cm^{-1}. The center of mass of the CH symmetric stretching band was calculated by integrating the top 10% of the intensity of the band. The baseline for integrating the top 10% of the intensity of the band was parallel to the OH-CH region baseline. The change in $\tilde{\nu}_{sym}$ versus temperature was used to characterize lipid phase transitions, as described previously (62). Because rotamers are either in *trans* or *gauche* conformations, phase transitions were fit to a two-state sigmoidal equation using Sigma plot 10 software (Systat Software, Inc., Chicago, IL):

$$\tilde{\nu}_{sym} = \left(\tilde{\nu}_{sym}\right)_{minimum} + \left[\left(\tilde{\nu}_{sym}\right)_{maximum} - \left(\tilde{\nu}_{sym}\right)_{minimum}\right] / \left[1 + \left(\text{temperature/Tc}\right)^{\text{hillslope}}\right] \quad \textit{(Eq. 1)}$$

The $\tilde{\nu}_{sym}$ is the frequency of the symmetric CH_2 stretching band near 2,850 cm^{-1}. Tc is the phase transition temperature. Hillslope is a measure of the degree to which one lipid influences the melting of adjacent lipids. The steeper the phase transition, the larger is the hillslope.

Lipid order at 25 and 33.4°C was calculated by extrapolating the $\tilde{\nu}_{sym}$ at 25 and 33.4°C from the fit of the phase transition and then converting $\tilde{\nu}_{sym}$ to the percentage of *trans* rotamers, a measure of lipid conformational order (62). The data for percentage of *trans* rotamer were used to calculate the phase-transition change in enthalpy (ΔH) and entropy (ΔS) from the slopes of Arrhenius plots (62).

Estimation of whale age

Three published methods for estimating the age of bowhead whales were used in this analysis (51, 52, 54). For this work, a mean and SE was not calculated, rather an age range was determined for each of the three animals and the pool of whales.

Statistics

Curves were fit using Sigma plot 10 software (Systat Software, Inc.) and the confidence levels, *P*, were obtained from a critical value table of the Pearson product-moment correlation coefficient. A value of $P < 0.01$ was considered statistically significant.

RESULTS

Bowhead whale eyes were collected from seven female and six male legally subsistence-harvested bowhead whales in 2011, 2013, 2014, and 2015. Total body length measured from the rostrum to the fluke notch ranged between 8.2 and 17.2 m. The length of four of the animals was greater than 13 m, thus they were mature (51). The demographic of the samples are summarized in **Table 1**.

NMR spectroscopy

^{31}P-NMR was used to quantify whale lens phospholipids (**Fig. 1**). The major phospholipids of the bowhead whale lens were sphingolipids, which composed 60% to 100% of the total phospholipid (Table 1). For two of the lenses, only one ^{31}P-NMR resonance for DHSM was visible. To confirm that the resonance assignment was correct, the sample was spiked with bovine SM and, indeed, the resonances for SM (−0.090 ppm) and DHSM (0.117 ppm) were in the correct position (Fig. 1iii) (63). The lenses from the two largest (13B1; 14B6) and thus oldest whales weighed the most and had the most DHSM (Table 1).

Cholesterol was quantitated from the ^{1}H-NMR spectra of the lens lipid extracts. Phospholipid was quantified from the amide NH resonances near 6.81 and 6.22 ppm (**Fig. 2B**) assigned to hydrated and partially hydrated sphingolipid, respectively (63, 64), and the resonance near 3.48 ppm (Fig. 2A) assigned to the head group N-CH_2 moiety (63–65). The assignments were reasonable as the resonances were in the correct position and the measured average NCH_2/amide-NH intensity ratio was 1.9, close to the expected intensity ratio of 2. Cholesterol was quantified from the CH_3 resonance near 0.67 ppm (Fig. 2C) assigned to carbon 18 and the CH resonance near 1.83 ppm (Fig. 2D) assigned to H1α, H2α, and H16α of the cholesterol molecule (66–68). A proton resonance from the cholesterol ester at 4.6 ppm was not detected, indicating that most or all of the cholesterol was not esterified. The assignments are reasonable, as the resonances were in the correct position and the measured (3 × CH)/CH_3 average intensity ratio was 0.96, close to the expected intensity ratio of 1. The four combinations of cholesterol/phospholipid intensity ratios had a relative SE of 4% for each sample (Table 1).

TABLE 1. Bowhead whale demographics and lens weight and phospholipid composition

					Mole Percent							
Sample	Gender	TBL (m)	Lens Weight (mg)	Age[a] (years)	PEe/PGe	DHS	PEe	PSe	SM	PCe	PC	C:PL (mole:mole)
A (13B1)	F	16.5	890	100–140	n.d.	100	n.d.	n.d.	n.d.	n.d.	n.d.	9.0 ± 0.2
B (14B6)	F	17.2	660	72–87	n.d.	100	n.d.	n.d.	n.d.	n.d.	n.d.	10.3 ± 0.6
C (11B9)	F	12.5	470	15–22	n.d.	27.7	n.d.	n.d.	72.3	n.d.	n.d.	9.1 ± 1.1
Pool (n = 10)	40% F	8.2–14.5	389 ± 270	<25	2.3	14.4	11.0	3.3	48.2	7.5	13.2	10.3 ± 0.5

C:PL, cholesterol:phospholipid; DHSM, dihydrosphingomyelin; PEe, phosphatidylethanolamine ether; PSe, phosphatidylserine ether; PCe, PC ether; PGe, phosphatidylglycerol ether; TBL, total body length; n.d., not detected. Data are expressed as values ± SEM.

[a]Age range estimated applying methods from (51, 52, 54).

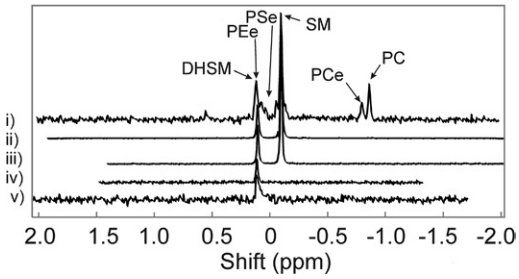

Fig. 1. ^{31}P-NMR spectra of phospholipids extracted from bowhead whale lenses. Spectra were used to quantify the phospholipid composition in Table 1. Pool (i), whale C (ii), whale A plus SM standard (iii), whale A (iv), Whale B (v). DHSM, dihydrosphpningomyelin; PEe, phosphatidylethanolamine ether; PSe, phosphatidylserine ether; PCe, PC ether.

The average molar cholesterol/phospholipid ratio for all four samples was similar, 10 ± 0.7 mol cholesterol per mole phospholipid (Table 1).

Infrared spectroscopy

Infrared spectroscopy was used to measure lipid-lipid interactions and the composition of whale lipid suspensions. The CH_2 stretching and bending bands were predominant in the infrared spectra of lipids due to the large number of CH_2 groups in their hydrocarbon chains (**Fig. 3**). Tentative infrared band assignments are listed in **Table 2**. Note that the intensity of the carbonyl band near 1,740 cm^{-1} is very small compared with the intensity of the amide band near 1,650 cm^{-1} and the CH_2 bending band near 1,470 cm^{-1}, which supports the large percentage of ether and amide linked hydrocarbon chains measured by ^{31}P-NMR (Fig. 3B). Note also the similarities between the spectrum of the whale lens lipid extract (Fig. 3Bi) and that of bovine brain SM (Fig. 3Bii) and cholesterol (Fig. 3Biii).

The CH stretching region near 2,900 cm^{-1}, is composed of six major bands (Fig. 3A) (62, 69). In this study, we used the $\tilde{\nu}_{sym}$ near 2,850 cm^{-1} to estimate the *trans* to *gauche* rotamer content of the hydrocarbon chains (Fig. 3A). The $\tilde{\nu}_{sym}$ increased with an increase in temperature and the number of *gauche* rotamers, concurrent with a decrease in intensity (**Fig. 4**) (69). Lipid phase transitions were quantified by fitting them to a four-parameter two-state sigmoidal equation, as described by Borchman et al. (62). The four parameters fitted were the minimum and maximum $\tilde{\nu}_{sym}$ in the phase transition that corresponded to the most ordered and disordered states, respectively, the transition temperature at which half of the lipid molecules underwent a phase change, and the relative cooperativity. The broader the phase transition, the smaller the absolute value of the cooperativity. Cooperativity describes how the order of a lipid influences that of neighboring lipids. The four phase-transition parameters necessary for defining the phase transition and other parameters calculated from the defining parameters are listed in **Table 3**.

Lipid order was measured close to the temperature of the lens, 33.4°C, by extrapolating the $\tilde{\nu}_{sym}$ at 33.4°C from the fit of the phase transition and then converting $\tilde{\nu}_{sym}$ to the percentage of *trans* rotamers (Table 3) (61). Lipid order at 25°C was also calculated (Table 3) because the temperature of whale lenses exposed to extremely low arctic temperatures could be lower than that for humans. The phase transition was relatively broad, which indicates that the cooperativity between lipids was low and changes in lipid order with temperature were minimal.

Recalculating phase transition parameters from previous studies

We have measured lens lipid phase transitions for lipids extracted from a number of species, including rabbit (70),

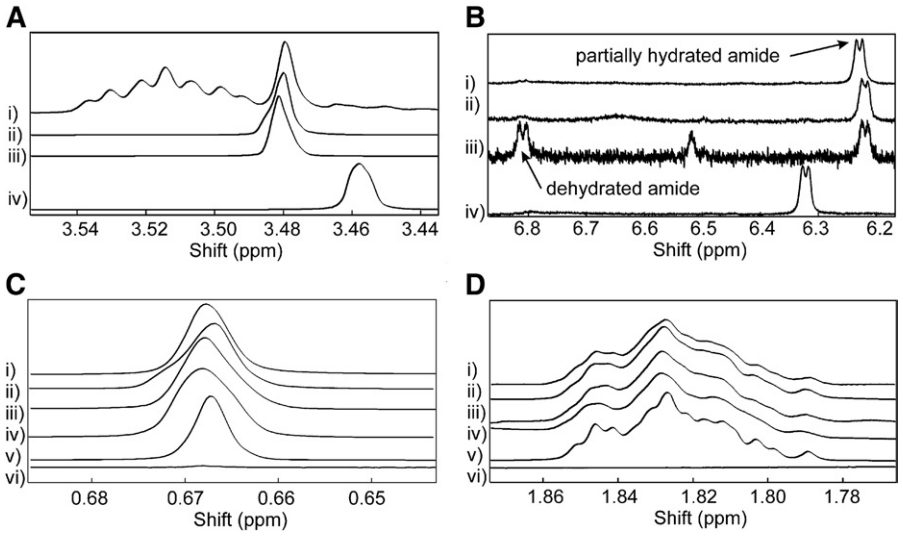

Fig. 2. ^{1}H-NMR spectra of lipids extracted from bowhead whale lenses. The spectra were used to quantify the molar cholesterol/phospholipid ratios of the extracts. Phospholipid was quantified from the amide NH resonances near 6.81 and 6.22 ppm (B) assigned to hydrated and partially hydrated sphingolipid, respectively, and the resonance near 3.48 ppm (A) assigned to the choline head group N-CH_2 moiety. Cholesterol was quantified from the CH_3 resonance near 0.67 ppm (C) assigned to carbon 18 and the CH resonance near 1.83 ppm (D) assigned to carbons 1, 2, and 16 of the cholesterol molecule.

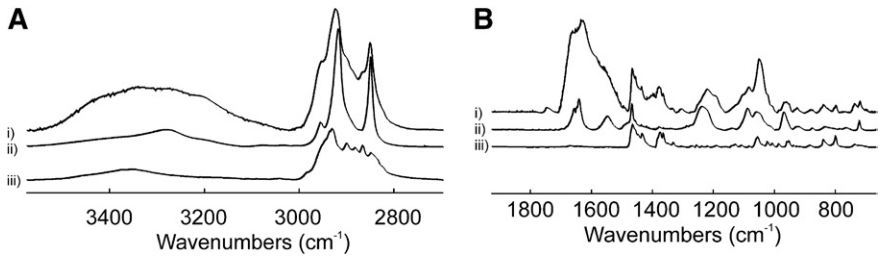

Fig. 3. Fourier transform infrared spectra of: bowhead whale lens lipid extract (i), bovine brain SM (ii), and cholesterol (iii). A: CH_2, OH, and amide A stretching region. B: Fingerprint region.

bovine (71), rat and camel (35), guinea pig (72), and humans (8, 73, 74). We refit the phase transition curves from previous studies and recalculated the percent *trans* rotamers because the four phase transition parameters used to define the whale lens lipid transition in the current study were not reported for other species. Also, in previous publications (35, 70–74), the equation used to curve fit the phase transitions was a general equation for sigmoidal curves. The equation 1 used in the current study is more physiologically relevant, as it is related to the "Hill" equation used to measure enzyme kinetics. Another reason to recalculate the previously measured phase transitions is the minimum and maximum $\tilde{\nu}_{sym}$ used in the older studies were less accurate. In previous studies (8, 35, 70–74), the maximum $\tilde{\nu}_{sym}$ of 2,854.5 cm^{-1} was estimated from phosphatidylcholine (PC) in $CHCl_3$. In this study, we used a maximum $\tilde{\nu}_{sym}$ of 2,855.36 cm^{-1} calculated from an isomeric distribution of hexanes (62). Also, in previous studies (8, 35, 70–74), the minimum $\tilde{\nu}_{sym}$ of 2,849 cm^{-1} was estimated from dipalmitoylphosphatidylcholine at −20°C. In this study, we used a minimum $\tilde{\nu}_{sym}$ of 2,848.00 cm^{-1} calculated from distearoylphosphatidylcholine at −50°C (62). The recalculated phase transition parameters are listed in **Table 4** for comparison with the phase transition parameters for whale lenses calculated in this study. Arrhenius plots used to calculate the ΔH and ΔS values from the lipid phase transitions were linear, with correlation coefficients greater than 0.998.

Lens growth

The average lens growth of the bowhead whale was 4.4 mg/year calculated from the slope of the linear relationship ($r = 0.539$, n = 13, $P < 0.05$) between lens weight and body length (0.0505 g/m) from the current study divided by the slope of the linear relationship ($r = 0.479$, n = 20, $P < 0.02$) between lens weight and age (11.48 years per meter) from (53).

Correlations

There was a strong linear correlation between the percentage of lens sphingolipid and lens lipid hydrocarbon chain order measured at 34.8°C (**Fig. 5A**, $r = 0.8911$, $P < 0.01$) until about 60% sphingolipid, above which there was little change in the hydrocarbon chain order. The percentage of lens sphingolipid correlated with lens lipid phase transition temperature (Fig. 5B, $r = 0.7241$, $P < 0.01$). The expected maximal lifespan of the whale was the longest of the species measured in this study and the percentage of whale lens sphingolipid fit well in the correlation between the percentage of lens sphingolipid and expected maximal lifespan measured in other studies (Fig. 5C, $r = 0.8980$, $P < 0.01$). The percentage of whale lens PC fit well in the correlation between the percentage of lens sphingolipid and expected maximal lifespan measured from other studies (Fig. 5D, $r = 0.9141$, $P < 0.01$). The percentage of DHSM was linearly related to total body length (Table 1, $r = 0.9942$, $P < 0.01$), the age of the whale (51, 52, 54), and estimated age (**Fig. 6**, $r = 1$, $P < 0.001$). Lipid order and the phase transition temperature were also linearly related ($r = 0.8911$, $P < 0.01$).

DISCUSSION

Most whale species have well developed eyes. Underwater and aerial vision is critical for foraging at various dive depths, predator avoidance, navigation, and recognition of other individuals. Bowhead whales are the only baleen whale native to the Arctic. They have a small palpebral fissure and a thick and fleshy palpebra with a thick overlaying epidermis (**Fig. 7** (75)). Compared with terrestrial mammals, the eyes of whales are well adapted to their light

TABLE 2. Tentative infrared band assignments

Lipid Band (cm^{-1})	Tentative Band Assignment
695–738	CH_2, rock
918	OH carboxylic acid
960	C-N-C
1,043	C-O, ester stretch
1,067	Symmetric stretch, PO_2^- groups
1,172	C-O
1,245	C-O
1,272	asymmetric stretch, PO_2^- groups
1,349	CH_2 wagging progression
1,366	CH_2 wagging progression
1,378	CH_2 wagging progression, C-H bend CH_3 groups
1,408	symmetric stretch, COO^- groups
1,469	C-H in-plane bend, CH_2 groups
1,650	Conjugated dienes
1,739	C=O, acyl linkage
2,950	symmetric stretch, CH_2
2,924	asymmetric stretch, CH_2 group
2,957	asymmetric stretch, CH_3 groups
3,010	C-H stretch, -HC=CH- moiety
3,208	OH stretch
3,348	OH stretch
3,453	OH stretch, O-O-H stretch

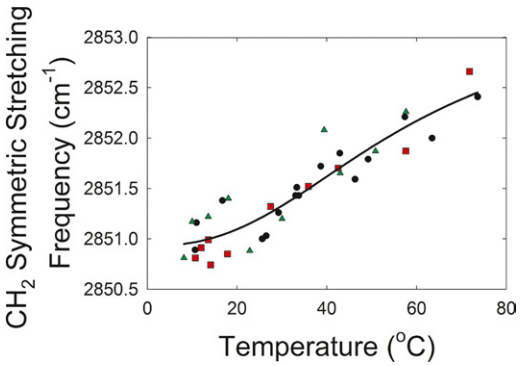

Fig. 4. Lipid phase transition of aqueous suspensions of bowhead whale lens lipids. Whale A (black circle), whale B (gray square), whale C (gray triangle), curve fit of all data to a four parameter sigmoidal curve (solid black line). Data from the fit are presented in Table 3. An increase in the stretching frequency is associated with an increase in hydrocarbon chain *trans* rotomers, disorder, and fluidity.

limited aquatic environment with a thick cornea, sclera, and choroid that protect their eyes from the mechanical stress of diving and the cold temperature of the arctic water (76). The reflective layer of tapetum lucidum almost completely covers the fundus, enabling whales to see in low light conditions and sense light scattered from plankton (77). In addition, adaptation of retinal pigments further enhances their ability to see under low light conditions (78). The lens of the bowhead whale is very important for focusing light onto the retina because, unlike terrestrial mammals, the cornea of the bowhead whale is not refractive in water and of little optical importance (75). The center of the large spherical lens is in the center of the eyecup so that light coming from any direction is focused on the retina (77). Although zonules connect the lens to the ciliary process, the bowhead whale eye has no ciliary muscles (75), so accommodation is accomplished by the displacement of the lens by changes in intraocular pressure (77). Important to this study is the fact that bowhead whales do not get cataracts (54).

The longer animals live, the longer they require clear lenses. One may ask the question, why do rats get cataracts at 2 years, dogs at 8 years, and humans at 60 years? Environmental causes (e.g., UV radiation, smoking) could contribute to some of the differences, however, ageing is the primary reason behind cataract development in various species. All of the species in Fig. 5C have diverse diets, optical water conditions, UV exposure, different accommodation processes, and other factors that could contribute to the variations observed in the figure; yet, the correlation between lens sphingolipid and lifespan is still significant. The phospholipid composition of adult lenses was reported in Fig. 5C. As discussed in the Introduction, with the progression of age, lens membranes of the species studied contain higher amounts of DHSM and lower amounts of PCs. In this study, we found this to be true of whales (Fig. 6) and their lens composition fits the curves in Fig. 5. Is this coincidental or does it have a scientific basis?

TABLE 3. Whale lens lipid phase transition parameters from Fig. 4

Parameter	Value
Minimum (cm^{-1})	2,850.9 ± 0.1
Maximum (cm^{-1})	2,854.3 ± 1
Transition temperature (°C)	57 ± 24
Cooperativity	2 ± 1
Order 25.8°C	56 ± 1
Order 33.4°C	53 ± 1
ΔEnthalpy (kcal/mole)	20.8 ± 0.3
ΔEntropy (kcal/mole/degree)	0.063 ± 0.001

We found that whale lenses have one of the highest sphingolipid contents of lenses from the species studied. Lens membranes with a high content of saturated sphingolipids, like bowhead whale lenses, are less susceptible to oxidation because there is relatively less oxygen in these ordered bilayers, as well as fewer double bonds to become oxidized (15, 79–83). In this study, we found that whale lens lipid composition and structure support the finding that lens lipid hydrocarbon order is directly related to the sphingolipid content and indirectly related to the PC content of the lenses of many animals (Fig. 5). Thus for the whale lens, a high saturated sphingolipid content and increased head group interactions cause the lipid hydrocarbon chain region to become more ordered (63, 64). As a consequence of higher lipid order, membranes may be less susceptible to oxidative damage because oxygen is five times more soluble in lipid membranes than it is in water (84–90). In addition, oxygen is five to ten times more soluble in fluid membranes (90), such as membranes low in sphingolipids, than it is in water.

Bowhead whale lenses have one of the highest levels of cholesterol measured for lenses. Above a molar cholesterol/phospholipid ratio of about two, cholesterol crystalline bilayer domains form (91, 92). Because the phospholipid domain of the whale lens membranes is saturated with cholesterol, "the physical properties of the phospholipid bilayer portion of lens lipid membranes constant and independent of changes in the PL [phospholipid] composition that occur with age" (91, p. 722). While cholesterol probably plays a minor role in determining lens membrane phospholipid structure (71, 91), it is likely to play a role in raft formation (93) and protein aggregation. One purpose of cholesterol in the lens may be to antagonize the binding of α-crystallin to lens membranes (94). It has been proposed that α-crystallin binding to lens membranes may serve as a "crystallization seed" for the binding of other proteins to the membrane, resulting in protein aggregation and light scattering (95). Thus, a high level of cholesterol in whale lenses could inhibit protein aggregation and cataract in whale lenses. It should be noted that for intact lens membranes, "… this beneficial effect of cholesterol on light scattering is compensated by the effect of integral membrane proteins" (91, p. 721). A high amount of cholesterol in the whale lens may also be important because cholesterol causes the lens membranes to be less permeable to oxygen, which may serve to keep oxygen in the outer regions of the lens long enough for the mitochondria to degrade it (96, 97).

The high dihydrosphingolipid to sphingolipid ratio, 100%, in the oldest whale lenses is similar to that for human lenses (80%, Ref. 98) and may inhibit lens growth. It

TABLE 4. Lens lipid phase transition parameters recalculated from previous publications

Lens Species	Min $\tilde{\nu}_{sym}$ (cm^{-1})	Max $\tilde{\nu}_{sym}$ (cm^{-1})	Tc (°C)	Coop	Order 25.8°C (% *trans*)	Order 33.4°C (% *trans*)	ΔH (kcal/mole)	ΔS (kcal/mole/degree)
Rat whole	2,851.2 ± 0.2	2,855.0 ± 0.2	32 ± 2	3.3 ± 0.7	40 ± 2	29 ± 2	104 ± 1	0.340 ± 0.004
Rabbit whole	2,849.5 ± 0.3	2,854.3 ± 0.3	26 ± 1	6 ± 2	48 ± 5	26 ± 5	189 ± 3	0.63 ± 0.01
Guinea pig equatorial	2,852.3 ± 0.1	2,853.9 ± 0.2	47 ± 5	4 ± 2	40 ± 2	37 ± 2	55.9 ± 0.9	0.175 ± 0.003
Guinea pig nuclear	2,852.20 ± 0.05	2,855.1 ± 0.5	65 ± 9	2.9 ± 0.5	40.3 ± 0.7	37.8 ± 0.7	55.9 ± 0.9	0.166 ± 0.003
Camel equatorial	2,850.51 ± 0.02	2,853.1 ± 0.1	34.9 ± 0.9	4.9 ± 0.5	59.5 ± 0.32	50.3 ± 0.3	58 ± 1	0.188 ± 0.004
Camel nuclear	2,850.27 ± 0.02	2,852.63 ± 0.05	36.5 ± 0.3	6.7 ± 0.3	66.3 ± 0.3	57.7 ± 0.3	65.7 ± 0.7	0.212 ± 0.002
Bovine cortex	2,851.7 ± 0.1	2,853.9 ± 0.2	26 ± 3	2.4 ± 0.6	36 ± 2	31 ± 21	55.9 ± 0.9	0.187 ± 0.003
Bovine nucleus	2,851.3 ± 0.1	2,853.0 ± 0.2	32 ± 3	3.1 ± 0.9	47 ± 1	43 ± 1	28.3 ± 0.7	0.093 ± 0.002
Human cortex 25 year	2,850.44 ± 0.08	2,854 ± 1	68 ± 20	2.3 ± 0.5	62 ± 1	58 ± 1	31 ± 1	0.092 ± 0.003
Human nucleus 25 year	2,850.37 ± 0.04	2,854.1 ± 0.1	45 ± 1	3.0 ± 1.6	59.9 ± 0.6	53.3 ± 0.6	41 ± 2	0.120 ± 0.008
Human cortex 70 year	2,850.17 ± 0.08	2,850.9 ± 0.08	50.2 ± 2	4.3 ± 0.7	68 ± 1	65 ± 1	30 ± 3	0.09 ± 0.01
Human nucleus 70 year	2,850.6 ± 0.1	2,854.4 ± 0.7	62 ± 7	3.7 ± 0.8	62 ± 1	59 ± 1	67 ± 1	0.171 ± 0.004

Data recalculated from previous studies: rabbit (70), bovine (71), rat and camel (35), guinea pig (72), and humans (8, 73, 74). Coop, cooperativity; Max, maximum; Min, minimum; Tc, phase transition temperature.

has been suggested that that "the high relative contents of DHSMs provide a biochemically inert matrix in which only small amounts of PCs and SMs and their metabolites, known to promote and arrest growth, respectively, are present" (98, p. 725). The high DHSM to sphingolipid ratio in the older whale lenses may slow multiplication and elongation of lens cells. For instance, the growth rate of cow and pig lenses with a relatively low ratio of DHSM is 100 and 50 mg/year, respectively, whereas the growth rate of human and whale lenses with a relatively high ratio of DHSM is 2.4 and 4.4 mg/year, respectively. A slow growth rate would be an important factor to keep the size of the whale lens from increasing to over the 200 year lifespan of the bowhead whale. It is interesting that the DHSM to sphingolipid ratio for the younger whale lenses ranged from 23% to 28%. This suggests that lens growth could be faster in younger whale lenses and that lens growth slows with age. The decline in the relative amount of SM with age in whale lenses is unique and suggests that sphingomyelinases that do not lyse DHSM are present in whale lenses or perhaps because SM contains more double bonds than DHSM and is preferentially degraded.

In summary, the long-lived bowhead whale exhibits a variety of lens adaptations that confer resistance to oxidation, thereby allowing these membranes to stay clear for a relatively longer time than is the case in many other species. The specialized lens chemical composition in combination with an adapted external eye anatomy provide the bowhead

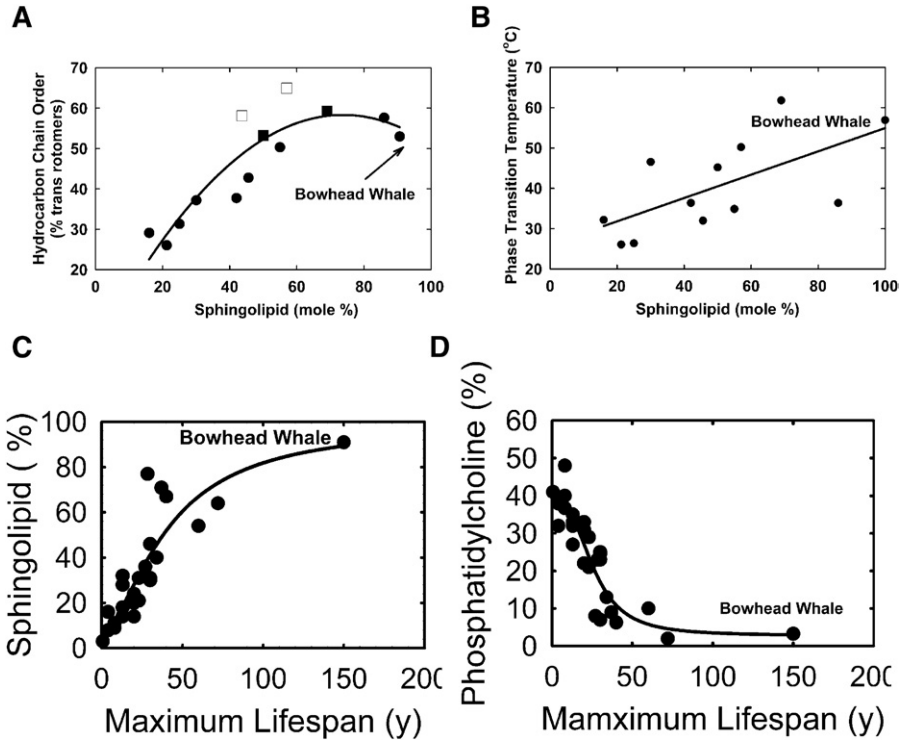

Fig. 5. A, B: Lipid phase transition parameters from Tables 3 and 4 and phospholipid composition data from (35) and the current study. C, D: Lifespan versus lipid phase transition parameters from Tables 3 and 4 and (35). Curve fitting (solid black line): hyperbola, single rectangular, two parameter (A); line (B); and four parameter logistic curve (C, D).

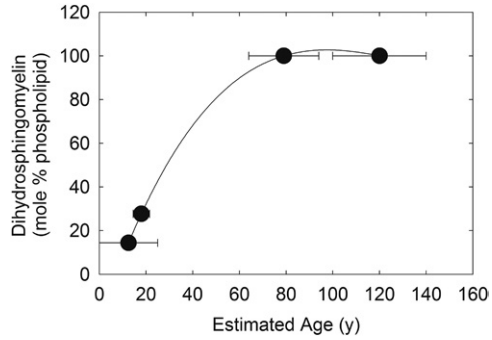

Fig. 6. Relationship between bowhead whale lens dihydrosphingomyelin content and estimated age. From Table 1. Linear curve fit, 3rd order ($r = 1$) (solid black line).

whales the evolutionary anatomical-physiological tools to protect and maintain vision for a long life under extreme arctic environmental conditions. The strong correlation between sphingolipid and lifespan may form a basis for future studies, which are needed because correlations do not infer cause. One could hope that if human lenses could be made to have a lipid composition similar to whales, like the bowhead whale, humans would not develop age-related cataracts for over 100 years.

The authors thank the whaling captains of Barrow, Alaska and the Alaska Eskimo Whaling Commission for allowing the sampling of subsistence-harvested bowhead whales and supporting the study. The authors thank Dr. Dana Wetzel of Mote Marine Laboratory and Dr. Susan Lubetkin at the University of Washington for their work estimating the age of bowhead whales, and the many field crew members for their support of the bio-monitoring sampling program of harvested bowhead whales, including Dave Ramey, Cyd Hanns, Rosemary McGuire, Hans Thewissen, Robert Suydam, Brian Person, Leslie Pierce, Todd Sformo, Leandra de Sousa, and Andrew van Duke.

Fig. 7. External eye anatomy of the bowhead whale showing a small palpebral fissure, thick and fleshy palpebra with a thick overlaying epidermis that protects the bowhead whales' eyes from the extreme arctic environmental conditions allowing them to maintain vision for their long, up to 200 year life. (Photo credit: North Slope Borough, Department of Wildlife Management, Utqiagvik, AK).

REFERENCES

1. Brian, G., and H. Taylor. 2001. Cataract blindness-challenges for the 21st century. *Bull. World Health Organ.* **79:** 249–256.
2. Truscott, R. J. 2005. Age-related nuclear cataract-oxidation is the key. *Exp. Eye Res.* **80:** 709–725.
3. Spector, A. 1984. The search for a solution to senile cataracts. Proctor lecture. *Invest. Ophthalmol. Vis. Sci.* **25:** 130–146.
4. Tang, D., D. Borchman, M. C. Yappert, and G. F. J. M. Vrenson. 2003. Influence of age, diabetes, and cataract on lipid-calcium and protein-calcium relationships in human lenses. *Invest. Ophthalmol. Vis. Sci.* **44:** 2059–2066.
5. Rhodes, J. D., and J. Sanderson. 2009. The mechanisms of calcium homeostasis and signalling in the lens. *Exp. Eye Res.* **88:** 226–234.
6. Borchman, D., and M. C. Yappert. 2010. Lipids and the ocular lens. *J. Lipid Res.* **51:** 2473–2488.
7. Borchman, D., Y. Ozaki, O. P. Lamba, W. C. Byrdwell, and M. C. Yappert. 1996. Age and regional structural characterization of clear human lens lipid membranes by infrared and near-infrared Raman spectroscopes. *Biospectroscopy.* **2:** 113–123.
8. Borchman, D., O. P. Lamba, and M. C. Yappert. 1993. Structural characterization of human lens membrane clear and cataractous lipid. *Exp. Eye Res.* **57:** 199–208.
9. Huang, L., V. Grami, Y. Marrero, D. Tang, M. C. Yappert, V. Rasi, and D. Borchman. 2005. Human lens phospholipid changes with age and cataract. *Invest. Ophthalmol. Vis. Sci.* **46:** 1682–1689.
10. Congdon, N., B. O'Colmain, C. C. Klaver, R. Klein, B. Muñoz, D. S. Friedman, J. Kempen, H. R. Taylor, and P. Mitchell; Eye Diseases Prevalence Research Group. 2004. Causes and prevalence of visual impairment among adults in the United States. *Arch. Ophthalmol.* **122:** 477–485.
11. Hughes, J. R., J. M. Deeley, S. J. Blanksby, F. Leisch, S. R. Ellis, R. J. Truscott, and T. W. Mitchell. 2012. Instability of the cellular lipidome with age. *Age (Dordr.).* **34:** 935–947.
12. Hughes, J. R., V. A. Levchenko, S. J. Blanksby, T. W. Mitchell, A. Williams, and R. J. Truscott. 2015. No turnover in lens lipids for the entire human lifespan. *Elife.* **4:** e06003.
13. Byrdwell, W. C., and D. Borchman. 1997. Liquid chromatography/mass-spectrometric characterization of sphingomyelin and dihydrosphingomyelin of human lens membranes. *Ophthalmic Res.* **29:** 191–206.
14. Deeley, J. M., J. A. Hankin, M. G. Friedrich, R. C. Murphy, R. J. Truscott, T. W. Mitchell, and S. J. Blanksby. 2010. Sphingolipid distribution changes with age in the human lens. *J. Lipid Res.* **51:** 2753–2760.
15. Oborina, E. M., and M. C. Yappert. 2003. Effect of sphingomyelin versus dipalmitoylphosphatidylcholine on the extent of lipid oxidation. *Chem. Phys. Lipids.* **123:** 223–232.
16. Huang, L., D. Tang, M. C. Yappert, and D. Borchman. 2006. Oxidation induced changes in human lens epithelial cells. 2. Mitochondria and the generation of reactive oxygen species. *Free Radic. Biol. Med.* **41:** 926–936.
17. Huang, L., M. C. Yappert, J. J. Miller, and D. Borchman. 2007. Thyroxine ameliorates oxidative stress by inducing lipid compositional changes in human lens epithelial cells. *Invest. Ophthalmol. Vis. Sci.* **48:** 3698–3704.
18. Huang, L., R. Estrada, M. C. Yappert, and D. Borchman. 2006. Oxidation induced changes in human lens epithelial cells. 1. Phospholipids. *Free Radic. Biol. Med.* **41:** 1425–1432.
19. Huang, L., M. C. Yappert, M. Jumblatt, and D. Borchman. 2008. Hyperoxia and thyroxine-treatment and the relationships between reactive oxygen species generation, mitochondrial membrane potential and cardiolipin in human lens epithelial cell cultures. *Curr. Eye Res.* **33:** 575–586.
20. Witting, L. A. 1965. Lipid peroxidation in vivo. *J. Am. Oil Chem. Soc.* **42:** 908–913.
21. Muller, F. L., M. S. Lustgarten, Y. Jang, A. Richardson, and H. Van Remmen. 2007. Trends in oxidative aging theories. *Free Radic. Biol. Med.* **43:** 477–503.
22. Balaban, R. S., S. Nemoto, and T. Finkel. 2005. Mitochondria, oxidants, and aging. *Cell.* **120:** 483–495.
23. McNulty, R., H. Wang, R. T. Mathias, B. J. Ortwerth, R. J. Truscott, and S. Bassnett. 2004. Regulation of tissue oxygen levels in the mammalian lens. *J. Physiol.* **559:** 883–898.
24. de Vries, A. C., M. A. Vermeer, A. L. Hendriks, H. Bloemendal, and L. H. Cohen. 1991. Biosynthetic capacity of the human lens upon aging. *Exp. Eye Res.* **53:** 519–524.

25. Borchman, D., and M. C. Yappert. 1998. Age-related lipid oxidation in human lenses. *Invest. Ophthalmol. Vis. Sci.* **39:** 1053–1058.
26. Bhuyan, K. C., and D. K. Bhuyan. 1984. Molecular mechanism of cataractogenesis: III. Toxic metabolites of oxygen as initiators of lipid peroxidation and cataract. *Curr. Eye Res.* **3:** 67–81.
27. Bhuyan, K. C., D. K. Bhuyan, and S. M. Podos. 1986. Lipid peroxidation in cataract of the human. *Life Sci.* **38:** 1463–1471.
28. Bhuyan, K. C., R. W. Master, R. S. Coles, and D. K. Bhuyan. 1986. Molecular mechanisms of cataractogenesis: IV. Evidence of phospholipid-malondialdehyde adduct in human senile cataract. *Mech. Ageing Dev.* **34:** 289–296.
29. Micelli-Ferrari, T., G. Vendemiale, I. Grattagliano, F. Boscia, L. Arnese, E. Altomare, and L. Cardia. 1996. Role of lipid peroxidation in the pathogenesis of myopic and senile cataract. *Br. J. Ophthalmol.* **80:** 840–843.
30. Simonelli, F., A. Nesti, M. Pensa, L. Romano, S. Savastano, E. Rinaldi, and G. Auricchio. 1989. Lipid peroxidation and human cataractogenesis in diabetes and severe myopia. *Exp. Eye Res.* **49:** 181–187.
31. Tomba, M. C., S. A. Gandolfi, and G. Maraini. 1984. Search for an oxidative stress in human senile cataract: hydrogen peroxide and ascorbic acid in the aqueous humour and malondialdehyde in the lens. *Lens Res.* **2:** 263–276.
32. Varma, S. D., D. Chand, Y. R. Sharma, J. F. Kuck, Jr., and D. Richards. 1984. Oxidative stress on lens and cataract formation: role of light and oxygen. *Curr. Eye Res.* **3:** 35–57.
33. Babizhayev, M. A., A. I. Deyev, and L. F. Linberg. 1988. Lipid peroxidation as a possible cause of cataract. *Mech. Ageing Dev.* **44:** 69–89.
34. Esterbauer, H., R. J. Schaur, and H. Zollner. 1991. Chemistry and biochemistry of 4-hydroxynonenal, malonaldehyde and related aldehydes. *Free Radic. Biol. Med.* **11:** 81–128.
35. Borchman, D., M. C. Yappert, and M. Afzal. 2004. Lens lipids and maximum lifespan. *Exp. Eye Res.* **79:** 761–768.
36. Podgor, M. J., G. H. Cassel, and W. B. Kannel. 1985. Lens changes and survival in a population-based study. *N. Engl. J. Med.* **313:** 1438–1444.
37. Klein, R., S. E. Moss, B. E. Klein, and D. L. DeMets. 1989. Relation of ocular and systemic factors to survival in diabetes. *Arch. Intern. Med.* **149:** 266–272.
38. Cohen, D. L., H. A. Neil, J. Sparrow, M. Thorogood, and J. L. Mann. 1990. Lens opacity and mortality in diabetes. *Diabet. Med.* **7:** 615–617.
39. Hirsch, R. P., and B. Schwartz. 1983. Increased mortality among elderly patients undergoing cataract extraction. *Arch. Ophthalmol.* **101:** 1034–1037.
40. Benson, W. H., M. E. Farber, and R. J. Caplan. 1988. Increased mortality rates after cataract surgery. A statistical analysis. *Ophthalmology.* **95:** 1288–1292.
41. Ninn-Pedersen, K., and U. Stenevi. 1995. Cataract patients in a defined Swedish population 1986-90: VII Inpatient and outpatient standardized mortality ratios. *Br. J. Ophthalmol.* **79:** 1115–1119.
42. Klein, R., B. E. Klein, and S. E. Moss. 1995. Age-related eye disease and survival. The Beaver Dam eye study. *Arch. Ophthalmol.* **113:** 333–339.
43. Borger, P. H., R. C. van Leeuwen, A. Hulsman, R. C. Wolfs, D. A. van der Kuip, V. Hofman, and P. T. de Jong. 2003. Is there a direct association between age-related eye diseases and mortality? The Rotterdam study. *Ophthalmology.* **110:** 1292–1296.
44. West, S. K., B. Munoz, J. Istre, G. S. Rubin, S. M. Friedman, L. P. Fried, K. Bandeen-Roche, and O. D. Schein. 2000. Mixed lens opacities and subsequent mortality. *Arch. Ophthalmol.* **118:** 393–397.
45. Thompson, J. R., J. M. Sparrow, J. M. Gibson, and A. R. Rosenthal. 1993. Cataract and survival in an elderly nondiabetic population. *Arch. Ophthalmol.* **111:** 675–679.
46. Hennis, A., S. Y. Wu, X. Li, B. Nemesure, and M. C. Leske; Barbados Eye Study Group. 2001. Lens opacities and mortality: the Barbados Eye Studies. *Ophthalmology.* **108:** 498–504.
47. Street, D. A., and J. C. Javitt. 1992. National five-year mortality after inpatient cataract extraction. *Am. J. Ophthalmol.* **113:** 263–268.
48. Williams, S. L., L. Ferrigno, P. Mora, F. Rosmini, and G. Maraini. 2002. Baseline cataract type and 10-year mortality in the Italian–American case control study of age-related cataract. *Am. J. Epidemiol.* **156:** 127–131.
49. Rozell, N. 2001. Bowhead whales may be the world's oldest mammals. Alaska Science Forum, article 1529. Geophysical Institute, University of Alaska Fairbanks, in cooperation with the UAF research community 2001. Available from: http://newsletter.gi.alaska.edu/node/5314
50. de Magalhães, J. P., and J. Costa. 2009. A database of vertebrate longevity records and their relation to other life-history traits. *J. Evol. Biol.* **22:** 1770–1774.
51. George, J. C., J. Bada, J. Zeh, L. Scott, S. Brown, T. O'Hara, and R. Suydam. 1999. Age and growth estimates of bowhead whales (Balaena mysticetus) via aspartic acid racemization. *Can. J. Zool.* **77:** 571–580.
52. George, J. C., E. Follmann, J. Zeh, M. Sousa, R. Tarpley, R. Suydam, and L. Horstmann-Dehn. 2011. A new way to estimate the age of bowhead whales (Balaena mysticetus) using ovarian corpora counts. *Can. J. Zool.* **89:** 840–852.
53. Zeh, J., G. J. Craig, B. Oliver, and M. Zauscher. 2013. Age and growth estimates of bowhead whales (Balaena mysticetus) via aspartic acid racemization. *Mar. Mamm. Sci.* **29:** 424–445.
54. Lubetkin, S. C., J. E. Zeh, and J. C. George. 2012. Statistical modeling of baleen and body length at age in bowhead whales (Balaena mysticetus). *Can. J. Zool.* **90:** 915–931.
55. Philo, L. M., E. B. Shotts, Jr., and J. C. George. 1993. Morbidity and mortality. *In* The Bowhead Whale. J. J. Burns, J. J. Montague, and C. J. Cowles, editors. Allen Press, Lawrence, KS. 275–307.
56. Zhao, L., X. L. Chen, J. Zhu, Y. B. Xi, X. Yang, L. D. Hu, H. Ouyang, S. H. Patel, X. Jin, D. Lin, et al. 2015. Lanosterol reverses protein aggregation in cataracts. *Nature.* **523:** 607–611.
57. Shanmugam, P. M., A. Barigali, J. Kadaskar, S. Borgohain, D. K. Mishra, R. Ramanjulu, and C. K. Minija. 2015. Effect of lanosterol on human cataract nucleus. *Indian J. Ophthalmol.* **63:** 888–890.
58. Philo, L. M., J. C. George, and T. F. Albert. 1992. Rope entanglement of bowhead whales (Balaena-mysticetus). *Mar. Mamm. Sci.* **8:** 306–311.
59. Byrdwell, W. C., H. Sato, A. K. Schwarz, D. Borchman, M. C. Yappert, and D. Tang. 2002. 31P NMR quantification and monophasic solvent purification of human and bovine lens phospholipids. *Lipids.* **37:** 1087–1092.
60. Meneses, P., and T. Glonek. 1988. High resolution 31P NMR of extracted phospholipids. *J. Lipid Res.* **29:** 679–689.
61. Estrada, R., A. Puppato, D. Borchman, and M. C. Yappert. 2010. Reevaluation of the phospholipid composition in membranes of adult human lenses by (31)P NMR and MALDI MS. *Biochim. Biophys. Acta.* **1798:** 303–311.
62. Borchman, D., G. N. Foulks, M. C. Yappert, and D. V. Ho. 2007. Temperature-induced conformational changes in human tearlipids hydrocarbon chains. *Biopolymers.* **87:** 124–133.
63. Ferguson-Yankey, S. R., D. Borchman, K. G. Taylor, D. B. DuPré, and M. C. Yappert. 2000. Conformational Studies of sphingolipids by NMR spectroscopy. I. Dihydrosphingomyelin. *Biochim. Biophys. Acta.* **1467:** 307–325.
64. Talbott, C. M., I. Vorobyov, D. Borchman, K. G. Taylor, D. B. DuPré, and M. C. Yappert. 2000. Conformational studies of sphingolipids by NMR spectroscopy. II. Sphingomyelin. *Biochim. Biophys. Acta.* **1467:** 326–337.
65. Sparling, M. L., R. Zidovetzki, L. Muller, and S. I. Chan. 1989. Analysis of membrane lipids by 500 MHz ^{1}H NMR. *Anal. Biochem.* **178:** 67–76.
66. Sawan, S. P., T. L. James, L. D. Gruenke, and J. C. Craig. 1979. Proton NMR assignments for cholesterol. Use of deuterium NMR as an assignment aid. *J. Magn. Reson.* **35:** 409–413.
67. Li, S., J. Pang, W. K. Wilson, and G. J. Schroepfer, Jr. 1999. Sterol synthesis. Preparation and characterization of fluorinated and deuterated analogs of oxygenated derivatives of cholesterol. *Chem. Phys. Lipids.* **99:** 33–71.
68. Muhr, P., W. Likussar, and M. Schubert-Zsilavecz. 1996. Structure investigation and proton and carbon-13 assignments of digitonin and cholesterol using multidimensional NMR techniques. *Magn. Reson. Chem.* **34:** 137–142.
69. Kóta, Z., M. Debreczeny, and B. Szalontai. 1999. Separable contributions of ordered and disordered lipid fatty acyl chain segments to nuCH_2 bands in model and biological membranes: a Fourier transform infrared spectroscopic study. *Biospectroscopy.* **5:** 169–178.
70. Delamere, N. A., C. A. Paterson, D. Borchman, K. L. King, and S. C. Cawood. 1991. Calcium transport, Ca-ATPase and lipid order in rabbit ocular lens membranes. *Am. J. Physiol.* **260:** C731–C737.
71. Borchman, D., R. I. Cenedella, and O. P. Lamba. 1996. Role of cholesterol in the structural order of lens lipids. *Exp. Eye Res.* **62:** 191–197.
72. Borchman, D., F. J. Gibblin, M. C. Yappert, V. R. Leverenz, V. N. Reddy, L. Lin, and D. Tang. 2000. Impact of aging and hyperbaric

oxygen in vivo on guinea pig lens lipid and nuclear light scatter. *Invest. Ophthalmol. Vis. Sci.* **41:** 3061–3073.
73. Borchman, D., P. Herrell, and M. C. Yappert. 1991. Structural characterization of human lens membrane lipid by infrared spectroscopy. *Invest. Ophthalmol. Vis. Sci.* **32:** 2404–2416.
74. Borchman, D., D. Tang, and M. C. Yappert. 1999. Lipid composition, membrane structure relationships in lens and muscle sarcoplasmic reticulum membranes. *Biospectroscopy.* **5:** 151–167.
75. Zhu, Q., D. J. Hillmann, and W. G. Henk. 2001. Morphology of the eye and surrounding structures of the bowhead whale, Balaena mystictus. *Mar. Mamm. Sci.* **17:** 729–750.
76. Rodrigues, F. M., F. M. Silva, A. C. Trompieri-Silva, J. E. Vergara-Parente, M. A. Miglino, and J. P. Guimarães. 2014. Morphology of the eyeball from the humpback whale (Megaptera novaeangliae). *Microsc. Res. Tech.* **77:** 348–355.
77. Mass, A. M., and A. Y. Supin. 2007. Adaptive features of aquatic mammals' eye. *Anat. Rec. (Hoboken).* **290:** 701–715.
78. Fasick, J. I., and P. R. Robinson. 2016. Adaptations of Cetacean retinal pigments to aquatic environments. *Front. Ecol. Evol.* **4:** 70.
79. Pamplona, R., M. Portero-Otin, D. Riba, C. Ruiz, J. Prat, J. M. Bellmunt, and G. Barja. 1998. Mitochondrial membrane peroxidizability index is inversely related to maximum life span in mammals. *J. Lipid Res.* **39:** 1989–1994.
80. Pamplona, R., M. Portero-Otin, R. J. Requena, S. R. Thorpe, A. Herroro, and G. Barja. 1999. A low degree of fatty acid unsaturation leads to lower lipid peroxidation and lipidoxidation-derived protein modification in heart mitochondria of the longevous pigeon than in the short-lived rat. *Mech. Ageing Dev.* **106:** 283–296.
81. Pamplona, R., M. Portero-Otin, C. Ruiz, R. Gredilla, A. Herroro, and G. Barja. 2000. Double bond content of phospholipids and lipid peroxidation negatively correlate with maximum longevity in the heart of mammals. *Mech. Ageing Dev.* **112:** 169–183.
82. Herrero, A., M. Portero-Otin, M. J. Bellmunt, R. Pamplona, and G. Barja. 2001. Effect of the degree of fatty acid unsaturation of rat heart mitochondria on their rates of H_2O_2 production and lipid and protein oxidative damage. *Mech. Ageing Dev.* **122:** 427–443.
83. Portero-Otín, M., J. M. Bellmunt, M. C. Ruiz, G. Barja, and R. Pamplona. 2001. Correlation of fatty acid unsaturation of the major liver mitochondrial phospholipid classes in mammals to their maximum life span potential. *Lipids.* **36:** 491–498.
84. Power, G. G., and H. Stegall. 1970. Solubility of gases in human red blood cell ghosts. *J. Appl. Physiol.* **29:** 145–149.
85. Kimmich, R., and A. Peters. 1975. Solvation of oxygen in lecthin bilayers. *Chem. Phys. Lipids.* **14:** 350–362.
86. Peters, A., and R. Kimmich. 1977. The heterogeneous solubility of oxygen in aqueous lecithin dispersions and its relation to chain mobility. A NMR relaxation and wide-line study. *Biophys. Struct. Mech.* **4:** 67–85.
87. Kimmich, R., A. Peters, and K. H. Spohn. 1981. Solubility of oxygen in lecithin bilayers and other hydrocarbon lamellae as a probe for free volume and transport properties. *J. Membr. Sci.* **9:** 313–336.
88. Subczynski, W. K., and J. S. Hyde. 1983. Concentration of oxygen in lipid bilayers using a spin-label method. *Biophys. J.* **41:** 283–286.
89. Vanderkooi, J. M., W. W. Wright, and M. Erecinska. 1990. Oxygen gradients in mitochondria examined with delayed luminescence from excited-state triplet probes. *Biochemistry.* **29:** 5332–5338.
90. Smotkin, E. S., F. T. Moy, and W. Z. Plachy. 1991. Dioxygen solubility in aqueous phosphatidylcholine dispersions. *Biochim. Biophys. Acta.* **1061:** 33–38.
91. Mainali, L., M. Raguz, W. J. O'Brien, and W. K. Subczynski. 2017. Changes in the properties and organization of human lens lipid membranes occurring with age. *Curr. Eye Res.* **42:** 721–731.
92. Jacob, R. F., R. J. Cenedella, and R. P. Mason. 1999. Direct evidence for immiscible cholesterol domains in human ocular lens fiber cell plasma membranes. *J. Biol. Chem.* **274:** 31613–31618.
93. Rujoi, M., J. Jin, D. Borchman, D. Tang, and M. C. Yappert. 2003. Isolation and lipid characterization of cholesterol-enriched fractions in cortical and nuclear human lens fibers. *Invest. Ophthalmol. Vis. Sci.* **44:** 1634–1642.
94. Tang, D., D. Borchman, R. J. Cenedella, and M. C. Yappert. 1998. Influence of cholesterol on the interaction of α-cystallin with phospholipid. *Exp. Eye Res.* **66:** 559–567.
95. Tang, D., D. Borchman, and M. C. Yappert. 1999. α-Crystallin-lens lipid interactions using resonance energy transfer. *Ophthalmic Res.* **31:** 452–462.
96. Widomska, J., M. Raguz, J. Dillon, E. R. Gaillard, and W. K. Subczynski. 2007. Physical properties of the lipid bilayer membrane made of calf lens lipids: EPR spin labeling studies. *Biochim. Biophys. Acta.* **1768:** 1454–1465.
97. Widomska, J., M. Raguz, and W. K. Subczynski. 2007. Oxygen permeability of the lipid bilayer membrane made of calf lens lipids. *Biochim. Biophys. Acta.* **1768:** 2635–2645.
98. Yappert, M. C., M. Rujoi, D. Borchman, I. Vorobyov, and R. Estrada. 2003. Glycero- versus sphingo-phospholipids in the control of mammalian lens growth. *Exp. Eye Res.* **76:** 725–734.